Accepted Manuscript

Discovery of the selective and efficacious inhibitors of FLT3 mutations

Yanle Zhi, Baoquan Li, Chao Yao, Hongmei Li, Puzhou Chen, Jiyin Bao, Tianren Qin, Yue Wang, Tao Lu, Shuai Lu

PII: S0223-5234(18)30501-4

DOI: 10.1016/j.ejmech.2018.06.010

Reference: EJMECH 10480

To appear in: *European Journal of Medicinal Chemistry*

Received Date: 6 February 2018

Revised Date: 4 May 2018

Accepted Date: 4 June 2018

Please cite this article as: Y. Zhi, B. Li, C. Yao, H. Li, P. Chen, J. Bao, T. Qin, Y. Wang, T. Lu, S. Lu, Discovery of the selective and efficacious inhibitors of FLT3 mutations, *European Journal of Medicinal Chemistry* (2018), doi: 10.1016/j.ejmech.2018.06.010.

FLT3/CDKs inhibitor		Selective FLT3 inhibitor
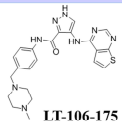	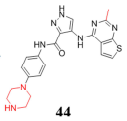	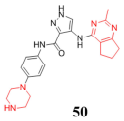
LT-106-175	**44**	**50**
FLT3: IC_{50} = 0.60 nM CDK2: IC_{50} = 9.10 nM CDK6: IC_{50} = 3.33 nM $T_{1/2}$: 51 min	FLT3: IC_{50} = 0.60 nM CDK2: IC_{50} = 81.54 nM CDK6: IC_{50} = 84.31 nM	FLT3: IC_{50} = 0.21 nM CDK2: 86.30% $^{\text{kinase activity at 0.123 μM}}$ CDK6: 91.25% $^{\text{kinase activity at 0.123 μM}}$ MV4-11: IC_{50} = 16 nM $T_{1/2}$: 147 min

Discovery of the selective and efficacious inhibitors of FLT3 mutations

Yanle Zhi[a,b], Baoquan Li[a], Chao Yao[a], Hongmei Li[a], Puzhou Chen[a], Jiyin Bao[a], Tianren Qin[c], Yue Wang[a], Tao Lu[*,a,b], Shuai Lu[*,a,b]

[a]School of Sciences, China Pharmaceutical University, 24 Tongjiaxiang, Nanjing 210009, PR China.

[b]State Key Laboratory of Natural Medicines, China Pharmaceutical University, 24 Tongjiaxiang, Nanjing 210009, PR China.

[c]School of Pharmacy, China Pharmaceutical University, 639 Longmian Avenue, Nanjing, 211198, PR China.

ABSTRACT

Fms-like tyrosine kinase 3 (FLT3) is among the most frequently mutated protein in acute myeloid leukemia (AML), which has been confirmed as an important drug target for AML chemotherapy. Starting from the lead compound LT-106-175, a series of 1-*H*-pyrazole-3-carboxamide derivatives were synthesized to improve the FLT3 inhibitory potency and selectivity. Among them, compound **50** was identified as a highly potent and selective FLT3 inhibitor (IC_{50} = 0.213 nM), which showed equal activities against various mutants of FLT3 including FLT3 (ITD)-D835V and FLT3 (ITD)-F691L that is resistant to quizartinib. Compound **50** also exhibited efficacy against the human AML cell line MV4-11 (IC_{50} = 16.1 nM) harboring FLT3-ITD mutants. Inversely, compound **50** displayed no cytotoxicity to FLT3-independent cells, and the biochemical analyses showed that its effects were related to the inhibition of FLT3 signal pathways. Additionally, compound **50** induced apoptosis in MV4-11 cell

as demonstrated by flow cytometry. Moreover, compound **50** showed enhanced metabolic stability. Altogether, it was concluded that compound **50** could be a promising FLT3 inhibitor for further developing therapeutic remedy of AML.

INTRODUCTION

Acute myeloid leukemia (AML) is characterized by the accumulation of a large number of abnormal cells that fail to differentiate into the functional granulocytes or monocytes[1]. Previous studies have found that elderly AML patients, which constitutes the majority of AML population, generally had poor outcomes, high healthcare expenditures, and median survival of <3 months[2]. Even with current treatments, as much as 70% of patients of 65 years old or older died of AML within 1 year after diagnosis[2]. Hence, effective treatment of AML in elderly patients still represents a severe challenge.

Fms-like tyrosine kinase 3 (FLT3), a member of the class III receptor tyrosine kinase family, is expressed by the immature hematopoietic cells, playing an important role in the proliferation, survival, and differentiation of multipotent stem cells[3]. However, FLT3 is over-expressed in 70% to 100% of AML cases[4-6] and mutation of FLT3 is the most common molecular alteration in AML[7]. Internal tandem duplication alteration (FLT3-ITD) in juxtamembrane portion is the most prevalent FLT3 mutation occurring in approximately 25% of those with de novo AML[7]. Point mutations in the kinase domain of the tyrosine (TKD) present in about 7% of AML cases[8, 9]. Both ITD and TKD are activating mutations, causing ligand-independent or constitutive activation of FLT3 signaling, and thereby promoting AML cell

survival and proliferation, which are often associated with poor prognosis[7], higher rate of relapse and reduced overall survival[8, 10-12]. Therefore, FLT3 has become an important target for AML[13, 14].

So far, a number of FLT3 inhibitors have been developed[15]. First-generation inhibitors, including sunitinib[16], sorafenib, midostaurin, lestaurtinib[17], and tandutinib[18], lack the specificity for FLT3. Consequently, their drug dosage and frequency of application may be limited by toxicity caused by the off-target activities; in turn, compromising the effectiveness of the treatment[19, 20]. Almost all of these compounds discontinued at phase II clinical trials, except midostaurin which was first approved by FDA for the treatment of AML[21]. Comparatively, the second-generation FLT3 inhibitors are more specific and potent, such as quizartinib[22] (phase III), which is still under active development. However, its c-Kit-inhibitory effect caused strong suppression of normal hematopoietic stem/progenitor cells[23]. Furthermore, some TKD mutations of FLT3 (D835Y, D835V, D835F, or F691L) could induce the resistant to quizartinib[24]. Thus, small-molecule inhibitors of FLT3 with strong potency against both FLT3-ITD and FLT3-TKD simultaneously and with high selectivity towards them hold great promise for more effective chemotherapy of AML. Here, we report the development of a new kind of FLT3 selective inhibitors against both FLT3-ITD and FLT3-TKD.

Chemistry

Scheme 1. Synthetic routes of compounds **33-41**.

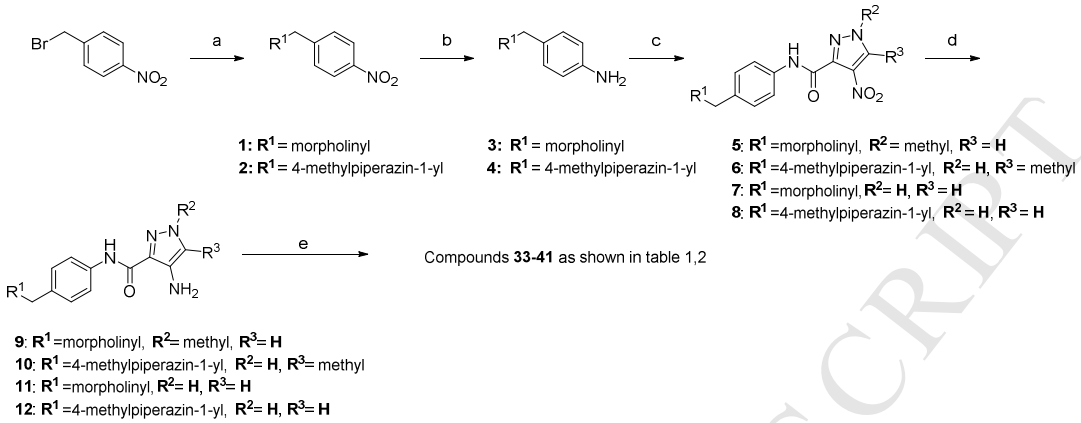

Reagents and conditions: (a) R^1-H, Et_3N, CH_2Cl_2; (b) FeO(OH)/C, 80% $NH_2NH_2{\cdot}H_2O$, 95% EtOH; (c) 4-Nitropyrazole-3-carboxylic acid or 1-methyl-4-nitro-1*H*-pyrazole-3-carboxylic acid or 5-methyl-4-nitro-1*H*-pyrazole-3-carboxylic acid, EDC·HCl, HOBt, DMF, r.t.; (d) FeO(OH)/C, 80% $NH_2NH_2{\cdot}H_2O$, 95% EtOH; (e) R^2-Cl, AcOH/H_2O.

Compounds **33-41** were prepared by the general approach shown in **Scheme 1**. 4-Nitrobenzyl bromide was used as the starting material to synthesize compounds **1** and **2** through a nucleophilic substitution reaction. Reduction of compound **1** and **2** with 80% hydrazine hydrate gave compounds **3** and **4**, which were then coupled with 4-nitropyrazole-3-carboxylic acid, 1-methyl-4-nitro-1H-pyrazole-3-carboxylic acid and 5-methyl-4-nitro-1H-pyrazole-3-carboxylic acid, respectively[25, 26][25, 26], to obtain compounds **5-8**. The same reduction method was used to convert compounds **5-8** to the corresponding amines **9-12.** The target compounds **33-41** were prepared by the direct ammonolysis of certain heterochorides with compounds **9-12**. Compounds **42-51** were prepared in a similar way (**Scheme 2**). Intermediates **13-15** were

synthesized by the nucleophilic substitution of 1-fluoro-4-nitrobenzene with the relative amines, and then the same procedures in **Scheme 1** were followed to give compounds **25-43**. Final compounds **44-51** were obtained upon the deprotection by acidic cleavage.

Scheme 2. Synthetic routes of compounds **42-51**.

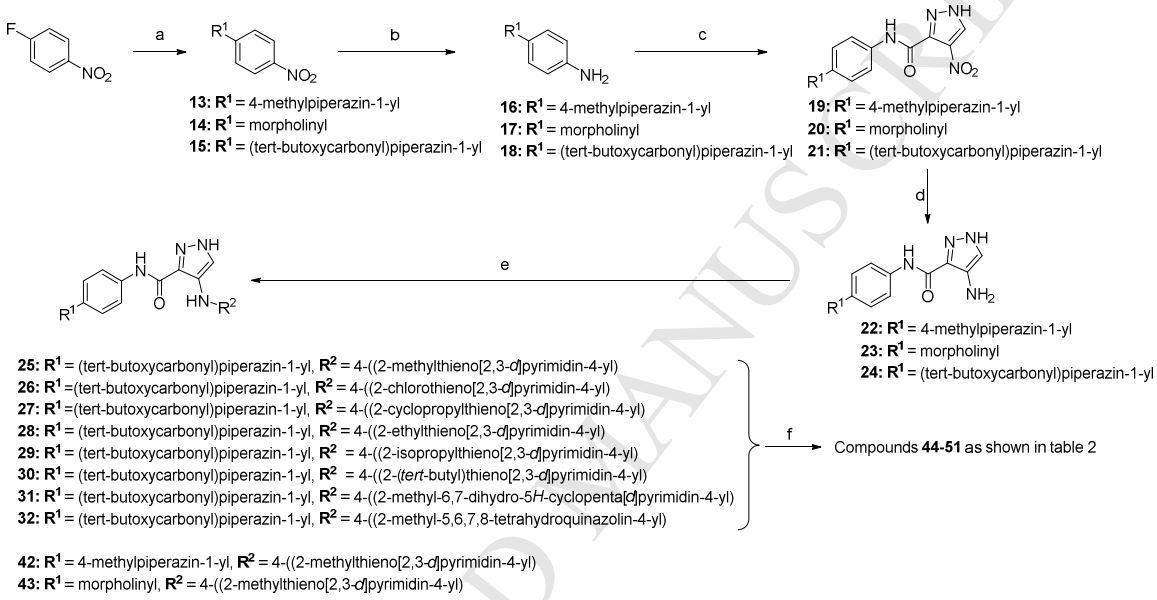

Reagents and conditions: (a) R^1-H, K_2CO_3, DMSO; (b) FeO(OH)/C, 80% $NH_2NH_2 \cdot H_2O$, 95% EtOH; (c) 4-Nitropyrazole-3-carboxylic acid or 1-methyl-4-nitro-1*H*-pyrazole-3-carboxylic acid or 5-methyl-4-nitro-1*H*-pyrazole-3-carboxylic acid, EDC·HCl, HOBt, DMF, r.t.; (d) FeO(OH)/C, 80% $NH_2NH_2 \cdot H_2O$, 95% EtOH; (e) R^2-Cl, AcOH/H_2O, 50 °C; (f) CF_3COOH, CH_2Cl_2.

RESULTS AND DISCUSSION

In our previous studies, a multiple kinases inhibitor LT-106-175 was discovered, which showed potent inhibitory activities against CDKs and FLT3. From the docking models of LT-106-175 with CDK2/6 and FLT3, we found that LT-106-175 interacted with CDK2/6 in the same manner. In the hinge area, the 1*H*-pyrazole-3-formyl motif formed three hydrogen bonds with the protein, and the fused thieno[2,3-d]pyrimidine ring was involved in the edge to face interaction with the gatekeeper residue Phe80/98, which played an important role in CDK2/6 inhibition[27, 28]. In the FLT3 model, three hydrogen bonds also presented between LT-106-175 and the hinge area; however the fused thieno[2,3-*d*]pyrimidine ring was far from reside Phe80, and the back pocket was bigger than that of CDK2/6. Thus, the back pocket of FLT3 could accommodate bulky groups. Therefore, we assumed that the introduction of some suitable groups to impede the edge to face interaction in CDK2/6 or to occupy more space in the back pocket of FLT3 would be beneficial for FLT3 selectivity. We hoped that the selectivity of this kind of compounds towards FLT3 could be enhanced through the sophisticated optimization guided by the assumption mentioned above, so that the potential side effects caused by CDK2 inhibition could be avoided[29].

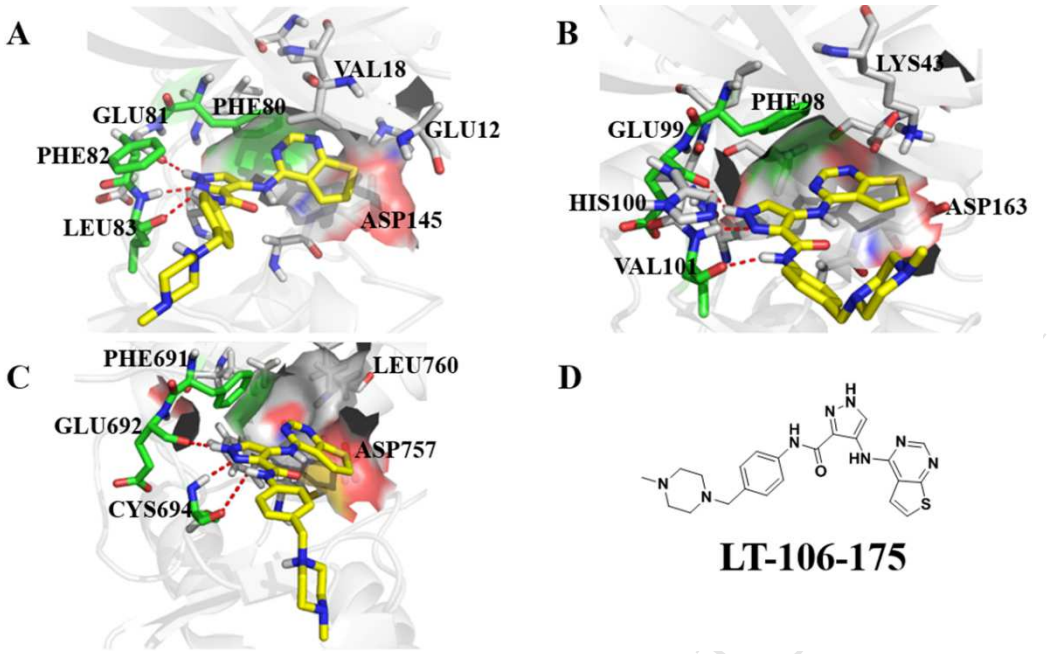

Figure 1. Molecular docking analysis of LT-106-175 bound to CDK2, CDK6 and FLT3 kinases. (A) Compound LT-106-175 docked into CDK2 (PDB code 2VU3). (B) Compound LT-106-175 docked into CDK6 (PDB code 2EUF). (C) Compound LT-106-175 docked into homology model of FLT3[30]. (D) Structure of compound LT-106-175.

As shown in **Table 1**, **Table 2** and **Table 3**, 19 new compounds were presented. All compounds were evaluated for their abilities to inhibit CDK2/6 and FLT3 at 0.123 μM firstly. Compounds that decreased the kinase activity by more than 80% were selected to further determine their half-maximal inhibitory concentration (IC_{50}) against CDK2/6 or FLT3. Additionally, we performed the growth-inhibition assays using human AML cell line MV4-11.

Methyl substitution onto the NH of pyrazole ring led to the total loss of activity against CDKs and FLT3 for compound **33**, which confirmed the importance of hydrogen bonds in the hinge region. Similarly, the introduction of a methyl group to

the C_5-position of pyrazole ring also eliminated the inhibitory activity against both CDK2/6 and FLT3 for compound **34**. However, compounds **36** and **37** showed great FLT3 selectivity over CDK2/6 when a methyl group was introduced to the pyrimidine ring, which was consistent with the assumption deduced from the molecule docking study. The IC_{50} value of compound **36** against FLT3 was 0.65 nM, which achieved almost 100-fold selectivity towards FLT3 over CDK2/6, and the anti-proliferative activity of compounds **36** and **37** against MV4-11 cell remained potent (IC_{50} = 0.052 nM and 0.062 nM, respectively), though the IC_{50} values decreased slightly when compared with LT-106-175. This indicated that high FLT3 selectivity of our compounds would not attenuate their cell activity significantly. Replacing the methyl in **36** with cyclopropyl (**38**) could improve the FLT3 selectivity over CDK2/6, but it also led to the 10-fold loss of potency against FLT3. Those data suggested that the methyl substitution at position 2 of pyrimidine was currently optimal. In order to investigate whether additional space exists for the introduction of groups, the isopropyl groups were adopted at C_2 position of thiophene (compounds **40** and **41**). Either the potency of FLT3 or the kinase selectivity was only maintained at the same level. (Table 1), but this result suggested that the modification on the thiophene ring was tolerated.

Table 1. Structures and biological data of compounds **33-41**

Compounds	Structure	(% enzyme activity) [a] /IC_{50} (nM) [b]			(% cell growth inhibition) [c] /IC_{50} (μM) [d]
		CDK2	CDK6	FLT3	MV4-11
LT-106-175	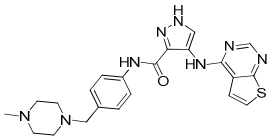	9.10 ± 0.16	3.33 ± 0.25	0.60 ± 0.11	0.016± 0.006
33	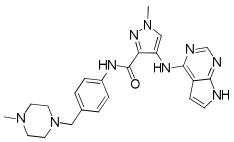	98.55 %	99.34 %	87.56%	nd[e]
34	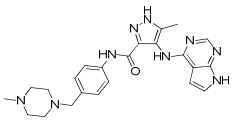	99.90 %	95.65 %	98.52 %	nd
35	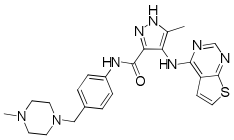	99.65 %	96.19 %	98.52 %	nd
36	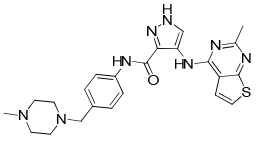	51.10 %	72.09 %	0.65 ± 0.02	0.052 ± 0.004
37	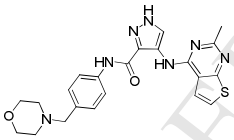	51.96 %	79.74 %	3.63 ± 0.11	0.062 ± 0.007
38	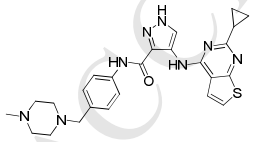	89.75 %	102.73 %	15.7 ± 0.33	0.061 ± 0.007
39	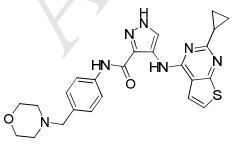	81.41 %	95.40 %	16.50 ± 0.45	0.078 ± 0.012
40	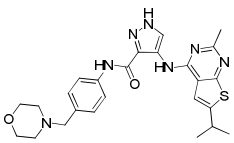	25.4 ± 0.57	33.21 ± 1.28	0.66 ± 0.13	0.048 ± 0.006

41	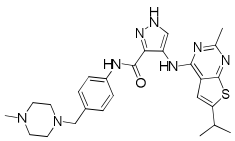	21.5 ± 0.64	19.24 ± 0.93	0.73 ± 0.27	0.065 ± 0.002

[a] % Enzyme activity at 0.123 μM in the presence of 10 μM ATP; [b] In the presence of 10 μM ATP, the values are the mean ± SD from three independent experiments. [c] % cell growth inhibition at 1 μM; [d] the highest test concentration is 1 μM, the values are the mean ± SD from three independent experiments. [e] nd: not determined

Varying the substitution in hydrophilic area helped us to identify which group was superior for the potency and selectivity of FLT3. Replacement of the 4-methylpiperazin in **36**, **38**, or **41** with morpholinyl (**37, 39** and **40**) was tolerated in terms of FLT3 potency and selectivity. Consistently, those compounds also kept moderate anti-proliferation activities in MV4-11 cell line. To our surprise, the introduction of the methylpiperazin-1-yl (**42**) and morpholinyl (**43**) directly onto the benzene ring could further improve FLT3 selectivity, indicating that the hydrophilic group also contributed to the FLT3 selectivity. Moreover, the potency of these two compounds against MV4-11 was also elevated mildly. Continuing modification on the 4-methylpiperazin gave compound **44**, from which methyl substitution was removed. Although this change was minor, compound **44** showed almost 131 times selectivity for FLT3 over CDK2/6, and its cell growth inhibitory activity was equal to LT-106-175. Overall, piperazin ring was the optimal hydrophilic group to achieve high FLT3 selectivity and inhibitory potency.

On the basis of the optimized hydrophilic group, SAR of various substitutions at pyrimidine ring was explored again. The activities against CDK2/6 decreased along

with the bulk increase of the substituted groups (Table 2), such as ethyl (**47**), isopropyl (**48**), tert-butyl (**49**), cyclopropyl (**46**) groups, etc. However, an obvious decrease in FLT3 kinase inhibition also occurred for those compounds (IC_{50}: 2.53-3.42 nM), accompanied by the reduction of cell activity, especially for compounds **49** bearing larger substituted group (IC_{50}: 20.5 nM). Only compound **45** with chlorine substitution exhibited maintained activities against FLT3 and MV4-11, which showed that the bulk of group was vital. These results proved that methyl group was the optimal option to keep the balance between FLT3 selectivity and cell potency.

Table 2. Optimization of the hydrophilic group and the gatekeeper group.

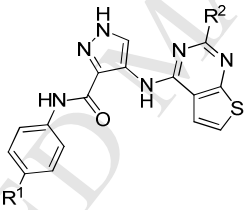

Compounds	**R^1**	**R^2**	**(% enzyme activity) [a] /IC_{50}(nM) [b]**			**(% cell growth inhibition) [c] /IC_{50} (μM) [d]**
			CDK2	**CDK6**	**FLT3**	**MV4-11**
42		-CH_3	71.23 %	72.74 %	0.95 ± 0.12	0.027 ± 0.003
43	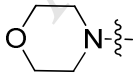	-CH_3	78.81 %	83.08 %	3.80 ± 0.18	0.033 ± 0.009
44	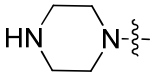	-CH_3	81.54 ± 1.23	84.31 ± 1.55	0.62 ± 0.04	0.019 ± 0.002
45	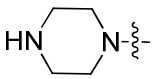	-Cl	56.82 %	63.57 %	0.47 ± 0.09	0.026 ± 0.006

46	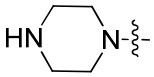		97.44 %	88%	2.53 ± 0.02	0.059 ± 0.005
47	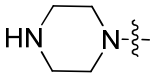		86.59%	87.04%	3.42 ± 0.12	0.065 ± 0.002
48	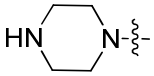		100.89%	93.50%	11.31 ± 0.21	0.057 ± 0.004
49	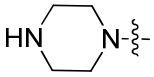		100.32%	99.21%	20.51 ± 0.42	0.098 ± 0.001

[a] % Enzyme activity at 0.123 μM in the presence of 10 μM ATP; [b] In the presence of 10 μM ATP with 0.123 μM compound, the values are the mean ± SD from three independent experiments. [c] % cell growth inhibition at 1 μM; [d] the highest test contraction is 1 μM, the values are the mean ± SD from three independent experiments. [e] nd: not determined

As reported, compounds with pyrimidothiophene ring are not metabolically stable *in vivo* [31, 32]. Our studies also confirmed that LT-106-175 was not stable in human liver microsomes ($t_{1/2}$: 51 min). Additionally, previous introduction of isopropyl to thiophene ring showed only a little influence on the kinase and cell activity (compound **40** and **41**). Hence, we chose to replace the thiophene ring directly with other heterocycles (data not shown) or saturated cycles. Among those compounds, compound **50** was obtained by replacing the thiophene (**44**) with cyclopentane ring, and it showed the highest inhibitory activity against FLT3 (IC_{50}: 0.213 nM). In addition, its selectivity for FLT3 also increased obviously when compared with compound **44**. Furthermore, compound **50** also had significant anti-proliferation activity in MV4-11 (IC_{50}: 0.016 μM). The similar replacement of thiophene with cyclohexane ring (**51**) did not affect the cell activity of compounds, but caused a slight decrease in FLT3 inhibitory activity as well as the selectivity for FLT3 (Table 3). In all, compound **50** was characterized to be the most potent and

selective FLT3 inhibitor in this study, with the remarkable anti-growth activity against MV4-11.

Table 3. Optimization of the thiophene ring in the hydrophobic pocket

Compounds	R^1	R^2	(% enzyme activity) [a] /IC_{50} (nM) [b]			(% cell growth inhibition) [c] /IC_{50} (μM) [d]
			CDK2	CDK6	FLT3	MV4-11
50	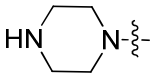	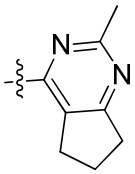	86.30%	91.25%	0.21 ± 0.05	0.016 ± 0.006
51	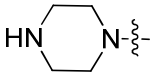	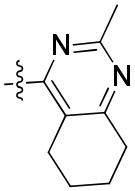	79.38%	87.22%	0.66 ± 0.03	0.018 ± 0.003

[a] % Enzyme activity at 0.123 μM in the presence of 10 μM ATP; [b] In the presence of 10 μM ATP with 0.123 μM compound, the values are the mean ± SD from three independent experiments. [c] % cell growth inhibition at 1 μM; [d] the highest test contraction is 1 μM, the values are the mean ± SD from three independent experiments.

Pharmacokinetics of compound 50 in Human Liver Microsomes

In order to verify whether the metabolic stability of compound **50** was improved, the human liver microsomes (HML) assay was performed. As data shown (**Table 4**), compound **50** was metabolically more stable ($t_{1/2}$: 147 min) than the lead compound **LT-106-175** ($t_{1/2}$: 51 min).

Table 4. Pharmacokinetics of compound **50** in human liver microsomes.

Human Liver Microsomes

Compound	$T_{1/2}$ (min)	CLint (μL/min/mg protein)	E_H (%)
LT-106-175	51	13.58	29.7
50	147	9.40	28.7

[a] $T_{1/2}$ is half life. [b] C_{Lint} is the intrinsic clearance. [c] liver uptake rate.

Kinase profiling

Through the structure-based optimization process, a relatively selective FLT3 inhibitor compound **50** was identified using a FLT3/CDK2/6 multiple kinase inhibitor as lead. Then, the selectivity profile of compound **50** was further characterized by the kinome assay on a panel of kinases. Thirty one kinases that were efficiently inhibited by LT-106-175 were selected (data have not been published). Generally, compound **50** displayed the highest inhibitory activity against FLT3 (98%) and little activity against CDKs. More importantly, compound **50** exhibited no inhibitory activity against c-Kit, which was usually vulnerable to other FLT3 inhibitors, such as PKC412 and AC220[33, 34]. Simultaneous inhibition of both FLT3 and c-Kit correlated with the myelosuppression toxicity observed from the most advanced clinical trials[23, 35]. Subsequently, kinases whose inhibitory rates exceed 50% were selected for IC_{50} determination. As shown in **Table 5**, compound **50** still showed excellent inhibitory activity against FLT3, the IC_{50} value of which was almost 120-fold stronger than that of FLT4/VEGFR3 (IC_{50}: 23.01 nM). Only weak inhibitory activity against FLT1/VEGFR1 (IC_{50}: 220.19 nM) and KDR/VEGFR2 (IC_{50}: 94.62 nM) was found. In comparison, LT-106-175 exhibit excellent inhibitory activity against CDK2/Cyclin A1,

CDK4/cyclinD1, CDK6/cyclinD1, FLT1/VEGFR1, ERK7/MAPK15, FLT4/VEGFR3 (IC_{50} < 10 nM) in addition to FLT3. All the data above confirmed that compound **50** was highly selective against FLT3 (**Figure 2**).

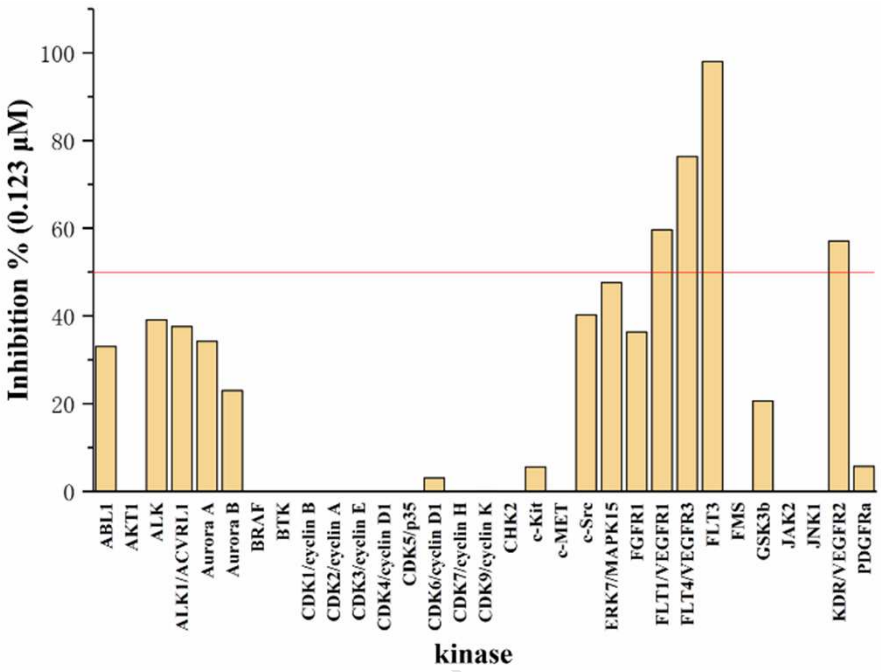

Figure 2. Kinase inhibition profile of compound **50** against 31 kinases.

Table 5. FLT3 selective inhibition by compound **50**

Kinase	Compound 50 (nM) [a]	LT-106-175	Staurosporine IC_{50} (M) [a]
FLT3	0.19 ± 0.04	0.60 ± 0.04	1.52 ± 0.21
FLT1/VEGFR1	220.19 ± 1.50	19.8 ± 0.43	15.97 ± 1.26
KDR/VEGFR2	94.62 ± 3.14	35.1 ± 1.56	1.67 ± 0.11
FLT4/VEGFR3	23.01 ± 2.31	4.5 ± 0.32	3.27 ± 0.36

[a] In the presence of 10 μM ATP, the IC_{50} are the mean ± SD from three independent experiments proceed by reaction biology company

Considering FLT3 mutation is very common and often indicates poor outcomes,

the efficacy of compound **50** against a variety of FLT3-ITD/TKD mutations was tested. As data shown in **Table 6**, compound **50** showed the significant inhibitory activity against those FLT3 mutants, even some of which were clinically identified as quizartinib-resistant, such as FLT3-D835Y, FLT3 (ITD)-F691L and FLT3 (ITD)-D835V[36, 37], etc. This indicated that compound **50** may be of promise to overcome the currently known drug resistances. It should be noted that lead compound LT-106-175 showed similar activity against those FLT3 mutants, indicating that the structural optimization did not affect FLT3 inhibitory potency eventually.

Table 6. The inhibitory activity of compound **50** against a panel of FLT3 mutants

Kinase	**Compound 50**	**Staurosporin**	**LT-106-175**
	IC_{50} / Kd (nM)	**IC_{50} (nM)**	**IC_{50} / Kd (nM)**
FLT3 (D835Y)	1.79 ± 0.04 [a]	0.71 ± 0.09	0.54 ± 0.03 [a]
FLT3 (F594_R595insR)	6.97 ± 0.08 [a]	1.74 ± 0.17	1.23 ± 0.10 [a]
FLT3 (F594_R595insREY)	9.15 ± 0.69 [a]	2.03 ± 0.26	7.35 ± 0.81 [a]
FLT3 (ITD)-NPOS	14.94 ± 1.51 [a]	5.49 ± 0.73	17.54 ± 2.43 [a]
FLT3 (ITD)-W51	12.85 ± 1.20 [a]	1.96 ± 0.25	1.85 ± 0.34 [a]
FLT3 (R595_E596)	8.74 ± 0.77 [a]	0.83 ± 0.09	2.67 ± 0.31 [a]
FLT3 (Y591-V592)	15.28 ± 1.24 [a]	4.95 ± 0.71	13.22 ± 1.15 [a]
FLT3(D835Y)	5.33 ± 0.49 [b]	nd[c]	7.01 ± 0.52 [b]
FLT3 (ITD)-D835V	3.70 ± 0.27 [b]	nd[c]	0.23 ± 0.11 [b]
FLT3 (ITD)-F691L	13.12 ± 0.92 [b]	nd[c]	1.30 ± 0.002 [b]

[a] In the presence of 10 μM ATP, the IC_{50} are the mean ± SD from three independent experiments proceed by reaction biology company. [b] Kd value provided by DiscoverX. [c] not tested

Molecular Modeling of Compound 50 with FLT3

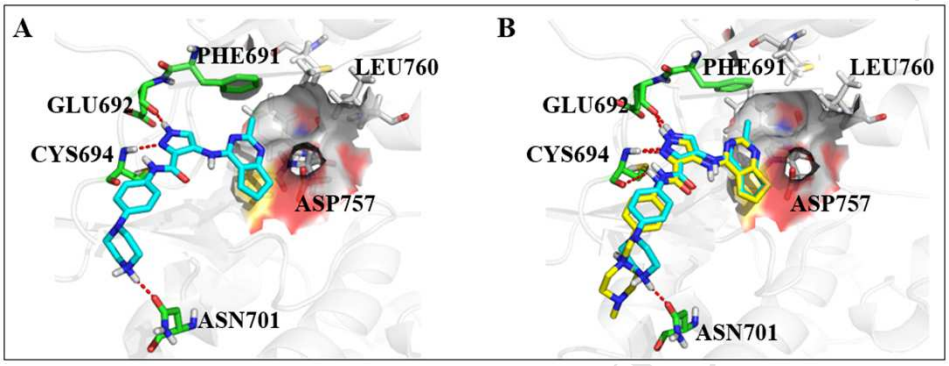

Figure 3. Molecular docking analysis of compound **50** bound to FLT3. (A) Compound **50** docked into homology model of FLT3. (B) Overlapping of the docked poses of compound **50** (Light blue) and LT-106-175 (yellow) in FLT3.

As one of the most selective FLT3 inhibitors in this series, compound **50** was docked into the homology model of FLT3 in order to explain the observed SAR. As shown in Figure 3, compound **50** adopted a similar binding mode with FLT3 as LT-106-175. The pyrazole ring bond to the kinase hinge region via two hydrogen bonds. In the hydrophilic pocket, the piperazine ring formed a hydrogen bond with Asn701, which helped improve the FLT3 inhibitory potency than other hydrophilic groups. The 6,7-dihydro-5H-cyclopenta[d]pyrimidine of compound **50** occupy the hydrophobic cavity. At the back of the ATP binding site the 2-methyl group made favorable van der waals interactions with the gatekeeper residue Phe691 around the back pocket. This further explains the result that introduction of methyl is the key factor to improve the selectivity for FLT3.

Cell activity

In assessing the anti-proliferative effect of compound **50** in other leukemia cell lines and lymphocytes cell lines, K562, MV4-11, MOLT-4, HL-60, MOLM-13 and Jurkat cell lines were selected for evaluation (**Table 7**). Consistent with its FLT3 inhibitory activity, FLT3-ITD-expressing cells exhibited extreme sensitivity to compound **50**. Compound **50** showed the most potent anti-proliferative activity against MV4-11 and MOLM-13 cells, with the IC_{50} value of 0.016 and 0.037 μM, respectively. Moreover, compound **50** had no efficacy in FLT3-low or FLT3–no expression cells, indicating that compound **50** may be less toxic against FLT3-independent cells *in vitro*.

Table 7. Effects of compound **50** on cell lines with different FLT3-expressing status

	IC_{50} (μM)[a]					
Cell line	**MV4-11**	**MOLM-13**	**MOLT-4**	**HL-60**	**K562**	**Jurkat**
FLT3 status	ITD	ITD	not known	WT/low[b]	FLT3-null[c]	FLT3-null
Compound 50	0.016 ± 0.005	0.037 ± 0.011	2.115 ± 0.981	26.690 ± 2.547	11.62 ± 1.280	4.595 ± 0.653
LT-106-175	0.016± 0.006	0.039 ± 0.002	NT	0.334[d]	0.235 [d]	NT

[a] The highest test contraction is 1 μM, the values are the mean ± SD from three independent experiments. [b] Cell line express less wide type FLT3. [c] cell lines not driven by oncogenic FLT3. [d] GI_{50} value were provided by NCI

Mechanism study

In order to further investigate whether the anti-AML activity is associated with the FLT3 inhibition and its downstream signaling proteins, we examined the effects of compound **50** on the phosphorylation of FLT3, STAT5, ERK and AKT in MV4-11 cells (**Figure 4**). As shown by Western blot assays, compound **50** could decrease the phosphorylation of FLT3 and its downstream signaling proteins, *i.e.* AKT, ERK and STAT5, in a dose-dependent manner. However, the down-regulatory effect of compound **50** on p-FLT3 at the concentration was not as strong as quizartinib (AC220). This may be due to relatively weak cell potency of compound **50** compared with quizartinib[38]. In conclusion, the anti-growth activity of compound **50** against MV4-11 was closely related to the inhibition of FLT3 signal pathway.

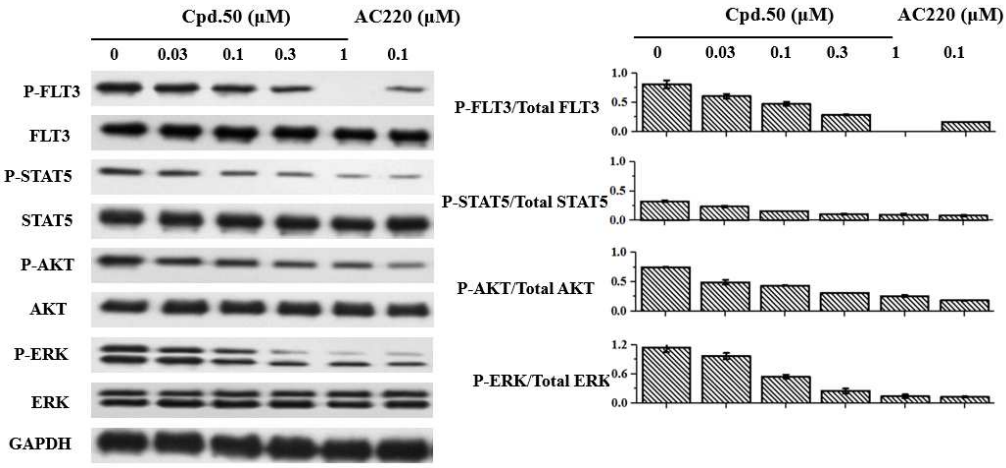

Figure 4. MV4-11 cells were treated with compound **50** or AC220 for 4 h, and the phosphorylation of FLT3, STAT5, ERK and AKT protein was analyzed by immune blotting.

In MV4-11 cell line, compound **50** induced cell apoptosis as detected by annexin V staining. A dose-dependent increase in the percentage of apoptotic cells was observed for compound **50**, which was consistent with AC220 (**Figure 5**).

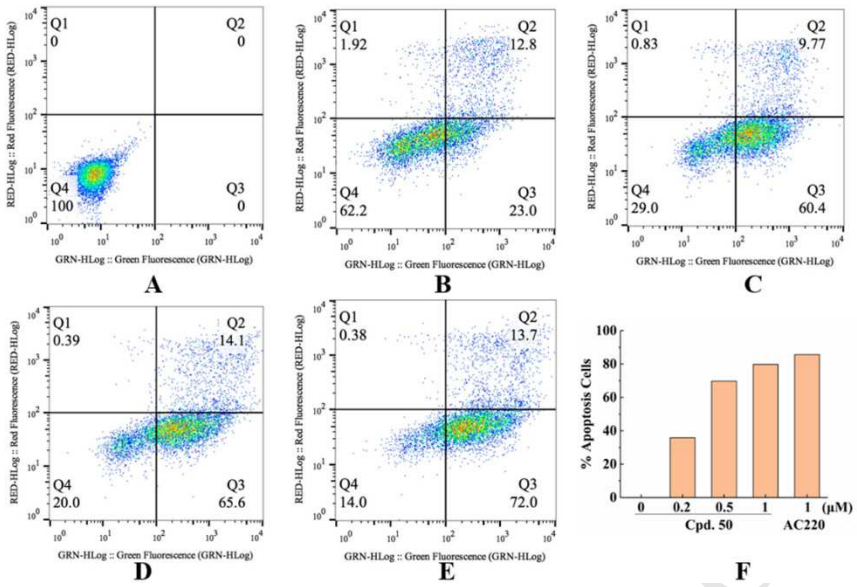

Figure 5. MV4-11 cells were treated with compound **50** for 24 h and then analyzed by Annexin V/PI staining. The percentage of cells undergoing apoptosis was defined as the sum of early apoptosis, advanced apoptosis and necrotic cells. (A) DMSO control; (B) compound **50** at 0.2 μM; (C) compound **50** at 0.5 μM; (D) compound **50** at 1 μM; (E) AC220 at 1 μM; (F) Percentage of apoptosis cells.

Conclusion

In summary, from the modification of a CDKs/FLT3 multi-kinase inhibitor LT-106-175 using the structure-guided drug design approach, a series of 1*H*-pyrazole-3-carboxamide derivatives were synthesized with the aim of improving the FLT3 selectivity. As one of the most potent mutated FLT3 inhibitor, compound **50** showed great selectivity for FLT3, especially without the inhibitory activity against c-Kit. Compound **50** also exhibited significant inhibitory efficacy to multiple FLT3 mutants, and thus it was expected to overcome the acquired resistance due to those mutations. Potent and selective growth inhibition activities were observed for compound **50** against the leukemia cell lines harboring FLT3-ITD mutant, such as

MV4-11 and MOLM-13, *in vitro*. We also preliminarily clarified that compound **50** indeed interfered FLT3 signal transduction in MV4-11 cell, and it induced apoptosis in a dose-dependent manner. Combining its selective inhibition of FLT3 mutants and FLT3-ITD expressing cells as well as the results from mechanism studies, it can be concluded that compound **50** may be a potential drug candidate for the treatment of AML.

EXPERMENTAL SECTION

General Procedures

Unless otherwise specified, reagents were purchased from commercial suppliers and used without further purification. Melting points were determined by X-4 digital display micro-melting point apparatus (Beijing Tech Instrument Co., Ltd.); NMR spectra were recorded on Bruker AVANCE AV-800 spectrometer (800 MHz for ^{1}H, 150 MHz for ^{13}C), Bruker AVANCE AV-600 spectrometer (600 MHz for ^{1}H, 126 MHz for ^{13}C) or Bruker AVANCE AV-300 spectrometer (300 MHz for ^{1}H, 75 MHz for ^{13}C); Mass spectra were obtained on the Agilent 1100 LC / MSD mass spectrometer (Agilent, USA) and Q-tofmicro MS (micromass company). All reactions were monitored by TLC (Merck Kieselgel GF254) and spots were visualized with UV light or iodine. The purity of biologically evaluated compounds was >95% as determined by HPLC.

General procedure A for the synthesis of compounds 9-12

4-Nitrobenzyl bromide (46.3 mmol) was dissolved in dichloromethane (100 mL). The solution was added to the mixture of relative amine (47.0 mmol) and

triethylamine (70.3 mmol) in dichloromethane (20 ml). The reaction mixture was stirred at r.t. for 24 h and was extracted with dichloromethane (100 ml × 3). After removal of the solvent, the residue was crystallized from ethanol, giving yellow powder. Compounds **1** and **2** were used for further reaction without purification.

To a suspension of compounds **1-2** (36.2 mmol) in 95% ethanol (100 ml), 85% $NH_2NH_2 \cdot H_2O$ (362 mmol), 95% ethanol (100 ml) and iron (III) oxide hydroxide (FeO(OH)/C, 2.0 g) were added and heated to reflux. When TLC analysis showed complete conversion of the starting material, the reaction mixture was filtrate through Cellit and the filtrate was concentrated in vacuum. The crude product was purified by silica gel colum chromatography (DCM/MeOH) to yield the title compound (**3** and **4**) as white solid.

The mixture of compound **4** (1eq, 18.5 mmol), 4-Nitro-1*H*-pyrazole-3-acid (1.1equiv, 20.4mmol), EDC (1.2equiv, 22.2mmol), HOBT (1.2equiv, 22.2mmol) in DMF (50 ml) was stirred for 24 hours. The ice water (100 ml) was added to the reaction mixture. A large amount of yellow solid precipitation (compound **8**) was acquired. Compound **8** was used without further purification. Compounds **8** was reduced by the same process as compound **4**, and then the resulting compound **12** was purified by column chromatography on silica gel, eluted with the appropriate solvent.

General procedure B for the synthesis of compounds 22-24

4-Fluoronitrobenzene (46.3 mmol) and K_2CO_3 were dissolved in DMSO (50 mL). The reaction mixture was stirred at r.t. for 30 min and then tert-butyl piperazine-1-carboxylate (69.5 mmol) was added. The reaction mixture was stirred at

70℃ for 5h. The ice water (500 ml) was added to the reaction mixture. A large amount of yellow solid precipitation (compound **13**) was acquired. Compound **13** was used for further reaction without purification. Compound **22** was synthesized by following the same synthetic process as the synthesis of compound **12.**

General procedure C for the synthesis of compounds 25-43

Compounds **9-12 or 22-24** (1 equiv.) and corresponding chorides (1.2 equiv.) in AcOH/H_2O:1/1 (20 ml) were heated to 50 °C. When TLC analysis showed the complete conversion of the starting material, sodium hydroxide (2 equiv.) was added to the mixture. Then, the reaction mixture was extracted with ethyl acetate. After removal of the solvent, compounds **33-43** were purified by column chromatography and the corresponding compounds were obtained. Compounds **25-32** were used without further purification.

General procedure D for the synthesis of compounds 44-51

Compound **25-32** (1 equiv.) were dissolved in dichloromethane/CF_3COOH and stirred at r.t. for 5 h. When TLC analysis showed complete conversion of the starting material, sodium hydroxide (2 equiv.) was added to the mixture. Then, the reaction mixture was extracted with dichloromethane. After removal of the solvent, the residue was purified by column chromatography, and the corresponding compounds were obtained.

4-((7H-pyrrolo[2,3-d]pyrimidin-4-yl)amino)-1-methyl-N-(4-((4-methylpiperazin-1-yl)methyl)phenyl)-1H-pyrazole-3-carboxamide (33). Compound **33** was prepared according to general procedure C on 0.5 mmol scale. Purification by column

chromatography (3% MeOH/DCM) yield the title compound (98 mg, 0.22 mmol Yield 44%). white solid; m.p 238-240 °C. HPLC analysis: retention time = 6.954 min; peak area, 98.55%. ^{1}H-NMR (300 MHz, DMSO-d_6) δ 11.95 (s, 1H), 10.28 (s, 1H), 9.58 (s, 1H), 8.60 (s, 1H), 8.39 (s, 1H), 7.79 (d, J = 8.1 Hz, 2H), 7.33 (s, 1H), 7.25 (d, J = 8.1 Hz, 2H), 6.49 (s, 1H), 4.03 (s, 3H), 3.42 (s, 2H), 2.36 (s, 6H), 2.17 (s, 3H). ^{13}C-NMR (126 MHz, DMSO-d_6) δ 162.82 (s), 151.94 (s), 151.61 (s), 151.09 (s), 137.51 (s), 134.05 (s), 131.99 (s), 129.53 (s), 125.73 (s), 123.64 (s), 123.23 (s), 121.14 (s), 103.59 (s), 97.18 (s), 62.10 (s), 55.10 (s), 52.80 (s), 46.03 (s). HRMS-EI m/z [M+H] $^{+}$ calcd for $C_{23}H_{28}N_9O$: 446.2417, found: 446.2386.

4-((7H-pyrrolo[2,3-d]pyrimidin-4-yl)amino)-5-methyl-N-(4-((4-methylpiperazin-1-yl)methyl)phenyl)-1H-pyrazole-3-carboxamide (34). Compound **34** was prepared according to general procedure C on 0.5 mmol scale. Purification by column chromatography (3% MeOH/DCM) yield the title compound (103 mg, 0.23 mmol Yield 46%). white solid; m.p 175-177 °C. HPLC analysis: retention time = 4.183 min; peak area, 98.77%. ^{1}H-NMR (300 MHz, DMSO-d_6) δ 11.65 (s, 1H), 10.02 (s, 1H), 8.73 (s, 1H), 8.07 (s, 1H), 7.63 (d, J = 7.9 Hz, 2H), 7.16 (m, 2H), 6.45 (s, 1H), 3.36 (s, 2H), 2.29 (s, 8H), 2.14 (d, J = 8.7 Hz, 6H). ^{13}C-NMR (151 MHz, DMSO-d_6) δ 155.99 (s), 151.56 (s), 151.31 (s), 138.01 (s), 133.59 (s), 129.51 (s), 122.06 (s), 120.04 (s), 119.16 (s), 103.38 (s), 99.25 (s), 62.11 (s), 55.17 (s), 52.93 (s), 46.19 (s). HRMS-EI m/z [M+H] $^{+}$ calcd for $C_{23}H_{28}N_9O$: 446.2417, found: 446.2383.

5-methyl-N-(4-((4-methylpiperazin-1-yl)methyl)phenyl)-4-(thieno[2,3-d]pyrimidin-4-ylamino)-1H-pyrazole-3-carboxamide (35). Compound **35** was prepared

according to general procedure C on 0.5 mmol scale. Purification by column chromatography (3% MeOH/DCM) yield the title compound (118 mg, 0.26 mmol, Yield 51%). white solid; m.p 92-94 °C. HPLC analysis: retention time = 4.961 min; peak area, 98.42%. ^{1}H-NMR (300 MHz, DMSO-d_6) δ 13.27 (s, 1H), 10.00 (s, 1H), 9.29 (s, 1H), 8.29 (s, 1H), 7.77 (s, 1H), 7.66 (d, J = 6.4 Hz, 3H), 7.17 (d, J = 8.2 Hz, 2H), 3.37 (s, 2H), 2.33 (s, 8H), 2.17 (d, J = 3.2 Hz, 6H). ^{13}C-NMR (151 MHz, DMSO-d_6) δ 166.68 (s), 157.09 (s), 154.02 (s), 138.04 (s), 133.45 (s), 129.49 (s), 123.66 (s), 120.20 (s), 120.09 (s), 118.22 (s), 116.97 (s), 62.04 (s), 55.02 (s), 52.72 (s), 45.97 (s), 21.61 (s). HRMS-EI m/z [M+H] $^{+}$ calcd for $C_{23}H_{27}N_8OS$: 463.2029, found: 463.2024.

N-(4-((4-methylpiperazin-1-yl)methyl)phenyl)-4-((2-methylthieno[2,3-d]pyrimidin-4-yl)amino)-1H-pyrazole-3-carboxamide (36). Compound **36** was prepared according to general procedure C on 0.5 mmol scale. Purification by column chromatography (5% MeOH/DCM) yield the title compound (112 mg, 0.24 mmol Yield 48%). white solid; m.p 270-272 °C. HPLC analysis: retention time = 3.990 min; peak area, 99.44%. ^{1}H-NMR (300 MHz, DMSO-d_6) δ 13.53 (s, 1H), 10.35 (s, 1H), 9.94 (s, 1H), 8.58 (s, 1H), 7.79 (d, *J* = 7.7 Hz, 2H), 7.67 (d, *J* = 5.8 Hz, 1H), 7.41 (d, *J* = 5.7 Hz, 1H), 7.26 (d, *J* = 8.1 Hz, 2H), 3.42 (s, 2H), 2.61 (s, 3H), 2.36 (s, 8H), 2.17 (s, 3H). ^{13}C-NMR (151 MHz, DMSO-d_6) δ 167.30 (s), 163.10 (s), 153.09 (s), 137.45 (s), 134.14 (s), 129.53 (s), 124.18 (s), 124.14 (s), 121.14 (s), 117.79 (s), 114.54 (s), 62.11 (s), 55.12 (s), 52.85 (s), 46.09 (s), 26.20 (s). HRMS-EI m/z [M+H] $^{+}$ calcd for $C_{23}H_{27}N_8OS$: 463.2029, found: 163.1995.

4-((2-methylthieno[2,3-d]pyrimidin-4-yl)amino)-N-(4-(morpholinomethyl)phenyl)-1H-pyrazole-3-carboxamide (37). Compound **37** was prepared according to general procedure C on 0.5 mmol scale. Purification by column chromatography (5% MeOH/DCM) yield the title compound (117 mg, 0.26 mmol Yield 52%). white solid; m.p 263-264 °C. HPLC analysis: retention time = 6.368 min; peak area, 98.44%. ^{1}H-NMR (300 MHz, DMSO-d_6) δ 13.51 (s, 1H), 10.37 (s, 1H), 9.93 (s, 1H), 8.59 (s, 1H), 7.80 (d, *J* = 8.3 Hz, 2H), 7.68 (d, *J* = 5.9 Hz, 1H), 7.41 (d, *J* = 6.0 Hz, 1H), 7.28 (d, *J* = 8.4 Hz, 2H), 3.58 (s, 4H), 3.43 (s, 2H), 2.61 (s, 3H), 2.35 (s, 4H). ^{13}C-NMR (151 MHz, DMSO-d_6) δ 167.30 (s), 163.10 (s), 153.07 (s), 137.53 (s), 133.68 (s), 133.37 (s), 129.63 (s), 124.17 (s), 124.14 (s), 121.26 (s), 121.15 (s), 117.78 (s), 114.54 (s), 66.67 (s), 62.52 (s), 53.61 (s), 26.20 (s). HRMS-EI m/z $[M+H]^+$ calcd for $C_{22}H_{24}N_7O_2S$: 450.1712, found: 450.1673.

4-((2-cyclopropylthieno[2,3-d]pyrimidin-4-yl)amino)-N-(4-((4-methylpiperazin-1-yl)methyl)phenyl)-1H-pyrazole-3-carboxamide (38). Compound **38** was prepared according to general procedure C on 0.5 mmol scale. Purification by column chromatography (5% MeOH/DCM) yield the title compound (95 mg, 0.20 mmol Yield 39%). yellow solid; m.p 138-139 °C. HPLC analysis: retention time = 7.091 min; peak area, 98.85%. ^{1}H-NMR (300 MHz, DMSO-d_6) δ 13.53 (s, 1H), 10.37 (s, 1H), 9.92 (s, 1H), 8.43 (s, 1H), 7.78 (d, *J* = 8.2 Hz, 2H), 7.62 (d, *J* = 5.9 Hz, 1H), 7.38 (d, *J* = 6.0 Hz, 1H), 7.26 (d, *J* = 8.2 Hz, 2H), 3.42 (s, 2H), 2.34 (s, 8H), 2.21 (s, 1H), 2.14 (s, 3H), 1.06 (m, 4H). ^{13}C-NMR (151 MHz, DMSO-d_6) δ 175.31 (s), 167.42 (s), 163.24 (s), 153.11 (s), 137.53 (s), 133.76 (s), 133.39 (s), 129.55 (s), 124.21 (s),

123.62 (s), 121.11 (s), 120.99 (s), 117.69 (s), 114.82 (s), 55.19 (s), 52.97 (s), 46.22 (s), 18.55 (s), 10.30 (s). HRMS-EI m/z $[M+H]^+$ calcd for $C_{25}H_{29}N_8OS$: 489.2185, found: 489.2165.

4-((2-cyclopropylthieno[2,3-d]pyrimidin-4-yl)amino)-N-(4-(morpholinomethyl)phenyl)-1H-pyrazole-3-carboxamide (39). Compound **39** was prepared according to general procedure C on 0.5 mmol scale. Purification by column chromatography (5% MeOH/DCM) yield the title compound (100 mg, 0.21 mmol Yield 41%). white solid; m.p 253-255 °C. HPLC analysis: retention time = 7.057 min; peak area, 100.00%. ^{1}H-NMR (300 MHz, DMSO-d_6) δ 13.51 (s, 1H), 10.36 (s, 1H), 9.92 (s, 1H), 8.44 (s, 1H), 7.80 (d, *J* = 7.9 Hz, 2H), 7.62 (d, *J* = 5.8 Hz, 1H), 7.37 (d, *J* = 6.0 Hz, 1H), 7.28 (d, *J* = 7.9 Hz, 2H), 3.57 (s, 4H), 3.43 (s, 2H), 2.35 (s, 4H), 2.21 (s, 1H), 1.07 (m, 4H). ^{13}C-NMR (126 MHz, DMSO-d_6) δ 167.43 (s), 167.36 (s), 163.14 (s), 153.09 (s), 137.52 (s), 133.74 (s), 133.31 (s), 129.65 (s), 124.26 (s), 123.60 (s), 121.17 (s), 120.75 (s), 117.78 (s), 114.73 (s), 66.68 (s), 62.53 (s), 53.61 (s), 18.54 (s), 10.38 (s). HRMS-EI m/z $[M+H]^+$ calcd for $C_{24}H_{26}N_7O_2S$: 476.1869, found: 476.1826.

4-((6-isopropyl-2-methylthieno[2,3-d]pyrimidin-4-yl)amino)-N-(4-(morpholinomethyl)phenyl)-1H-pyrazole-3-carboxamide (40). Compound **40** was prepared according to general procedure C on 0.5 mmol scale. Purification by column chromatography (5% MeOH/DCM) yield the title compound (135 mg, 0.28 mmol Yield 55%). white solid; m.p 263-264 °C. HPLC analysis: retention time = 3.750 min; peak area, 98.43%. ^{1}H-NMR (300 MHz, DMSO-d_6) δ 13.50 (s, 1H), 10.33 (s, 1H), 9.75 (s, 1H), 8.57 (s, 1H), 7.79 (d, *J* = 7.9 Hz, 2H), 7.28 (d, *J* = 8.1 Hz, 2H), 7.07 (s,

1H), 3.57 (s, 4H), 3.42 (s, 2H), 3.30 (m, 1H), 2.58 (s, 3H), 2.34 (s, 4H), 1.34 (d, *J* = 6.8 Hz, 6H). ^{13}C-NMR (151 MHz, DMSO-d_6) δ 163.15 (s), 162.34 (s), 152.27 (s), 150.04 (s), 137.50 (s), 133.68 (s), 133.17 (s), 129.61 (s), 124.34 (s), 121.23 (s), 114.54 (s), 111.94 (s), 66.67 (s), 62.52 (s), 53.60 (s), 30.51 (s), 26.15 (s), 24.61 (s). HRMS-EI m/z [M+H] $^{+}$ calcd for $C_{25}H_{30}N_7O_2S$: 492.2182, found: 492.2029..

4-((6-isopropyl-2-methylthieno[2,3-d]pyrimidin-4-yl)amino)-N-(4-((4-methylpiperazin-1-yl)methyl)phenyl)-1H-pyrazole-3-carboxamide (41). Compound **41** was prepared according to general procedure C on 0.5 mmol scale. Purification by column chromatography (5% MeOH/DCM) yield the title compound (115 mg, 0.23 mmol Yield 45%). white solid; m.p 151-153 °C. HPLC analysis: retention time = 7.214 min; peak area, 98.39%. ^{1}H-NMR MHz, (300 MHz, DMSO-d_6) δ 13.50 (s, 1H), 10.33 (s, 1H), 9.75 (s, 1H), 8.57 (s, 1H), 7.79 (d, *J* = 7.9 Hz, 2H), 7.28 (d, *J* = 8.1 Hz, 2H), 7.07 (s, 1H), 3.57 (s, 4H), 3.42 (s, 2H), 3.30 (m, 1H), 2.58 (s, 3H), 2.34 (s, 4H), 1.34 (d, *J* = 6.8 Hz, 6H). ^{13}C-NMR (151 MHz, DMSO-d_6) δ 166.03 (s), 162.34 (s), 152.31 (s), 150.02 (s), 137.76 (s), 129.77 (s), 124.36 (s), 121.21 (s), 114.53 (s), 111.98 (s), 61.31 (s), 53.69 (s), 50.80 (s), 43.98 (s), 30.51 (s), 26.16 (s), 24.61 (s). HRMS-EI m/z [M+H] $^{+}$ calcd for $C_{26}H_{33}N_8OS$: 505.2498, found: 505.2463.

N-(4-(4-methylpiperazin-1-yl)phenyl)-4-((2-methylthieno[2,3-d]pyrimidin-4-yl)amino)-1H-pyrazole-3-carboxamide (42). Compound **42** was prepared according to general procedure C on 0.5 mmol scale. Purification by column chromatography (5% MeOH/DCM) yield the title compound (112 mg, 0.25 mmol Yield 49%). yellow solid; m.p >269 °C. HPLC analysis: retention time = 6.587 min; peak area, 98.83%.

^{1}H-NMR (300 MHz, DMSO-d_6) 13.46 (s, 1H)，10.14 (s, 1H)，10.00 (s, 1H)，8.56 (s, 1H)，7.67 (m, J = 7.3, 4.1 Hz, 3H)，7.40 (d, J = 5.9 Hz, 1H)，6.93 (d, J = 9.0 Hz, 2H)，3.33 (s, 4H)，3.12 (s, 4H)，2.61 (s, 3H)，2.26 (s, 3H)．^{13}C-NMR (151 MHz, DMSO-d_6) δ 167.25 (s), 163.10 (s), 162.67 (s), 153.00 (s), 148.14 (s), 133.16 (s), 130.40 (s), 124.12 (s), 124.09 (s), 122.40 (s), 121.26 (s), 117.71 (s), 115.88 (s), 114.52 (s), 55.06 (s), 48.88 (s), 46.20 (s), 26.21 (s)．HRMS-EI m/z [M+H] $^{+}$ calcd for $C_{22}H_{25}N_8OS$: 449.1872, found: 449.1829.

4-((2-methylthieno[2,3-d]pyrimidin-4-yl)amino)-N-(4-morpholinophenyl)-1H-pyrazole-3-carboxamide (43). Compound **43** was prepared according to general procedure C on 0.5 mmol scale. Purification by column chromatography (5% MeOH/DCM) yield the title compound (96 mg, 0.22 mmol Yield 43%). yellow solid; m.p >310 °C. HPLC analysis: retention time = 6.444 min; peak area, 99.11%. ^{1}H-NMR (300 MHz, DMSO-d_6) δ13.44 (s, 1H)，10.16 (s, 1H), 10.00 (s, 1H), 8.57 (s, 1H), 7.69 (s, 3H), 7.40 (s, 1H), 6.94 (d, J = 7.4 Hz, 2H), 3.75 (s, 4H), 3.08 (s, 4H), 2.62 (s, 4H). ^{13}C-NMR (151 MHz, DMSO-d_6) δ 163.02 (s), 153.06 (s), 148.09 (s), 133.45 (s), 130.79 (s), 124.21 (s), 123.96 (s), 122.40 (s), 121.22 (s), 117.80 (s), 115.74 (s), 114.57 (s), 66.55 (s), 49.34 (s), 26.08 (s). HRMS-EI m/z [M+H] $^{+}$ calcd for $C_{21}H_{22}N_7O_2S$: 436.1556, found: 436.1511.

4-((2-methylthieno[2,3-d]pyrimidin-4-yl)amino)-*N*-(4-(piperazin-1-yl)phenyl)-1*H*-pyrazole-3-carboxamide (44). Compound **44** was prepared according to general procedure D on 0.5 mmol scale. Purification by column chromatography (5% MeOH/DCM) yield the title compound (63 mg, 0.15 mmol Yield 29%). white solid;

m.p >270 °C. HPLC analysis: retention time = 3.512 min; peak area, 99.22%. ^{1}H-NMR (300 MHz, DMSO-d_6) δ13.45 (s, 1H), 10.14 (s, 1H), 10.00 (s, 1H), 8.56 (s, 1H), 7.66 (s, 3H), 7.40 (d, J = 5.9 Hz, 1H), 6.93 (d, J = 8.7 Hz, 2H), 3.07 (s, 5H), 2.91 (s, 4H), 2.61 (s, 3H). ^{13}C-NMR (126 MHz, DMSO-d_6) δ 167.29 (s), 163.13 (s), 153.06 (s), 148.80 (s), 133.15 (s), 130.37 (s), 124.12 (s), 122.43 (s), 121.48 (s), 117.74 (s), 115.93 (s), 114.54 (s), 50.06 (s), 45.95 (s), 26.21 (s). HRMS-EI m/z [M+H] $^{+}$ calcd for $C_{21}H_{23}N_8OS$: 435.1716, found: 435.1676.

4-((2-chlorothieno[2,3-d]pyrimidin-4-yl)amino)-N-(4-(piperazin-1-yl)phenyl)-1H-pyrazole-3-carboxamide (45). Compound **45** was prepared according to general procedure D on 0.5 mmol scale. Purification by column chromatography (5% MeOH/DCM) yield the title compound (75 mg, 0.17 mmol Yield 33%). white solid; m.p >265 °C. HPLC analysis: retention time = 3.776 min; peak area, 99.32%. ^{1}H-NMR (300 MHz, DMSO-d_6) δ10.25 (s, 1H), 8.36 (s, 1H), 7.66 (t, J = 40.0 Hz, 5H), 6.94 (s, 2H), 3.07 (s, 4H), 2.91 (s, 4H). ^{13}C-NMR (151 MHz, DMSO-d_6) δ 122.34 (s), 116.55 (s), 47.07 (s), 43.66 (s), 41.80 – 40.19 (m), 40.12 (s), 40.03 (d, J = 21.0 Hz), 39.82 (s), 39.68 (s), 39.54 (s). HRMS-EI m/z [M+H] $^{+}$ calcd for $C_{20}H_{20}ClN_8OS$: 455.1169, found: 455.1134.

4-((2-cyclopropylthieno[2,3-d]pyrimidin-4-yl)amino)-N-(4-(piperazin-1-yl)phenyl)-1H-pyrazole-3-carboxamide (46). Compound **46** was prepared according to general procedure D on 0.5 mmol scale. Purification by column chromatography (5% MeOH/DCM) yield the title compound (71 mg, 0.16 mmol Yield 31%). white solid; m.p 68-69 °C. HPLC analysis: retention time = 4.007 min; peak area, 99.21%.

^{1}H-NMR (300 MHz, DMSO-d_6) δ 10.20 (s, 1H), 10.02 (s, 1H), 8.44 (s, 1H), 7.66 (dd, J = 21.3, 7.1 Hz, 3H), 7.37 (d, J = 5.7 Hz, 1H), 6.93 (d, J = 8.3 Hz, 2H), 3.04 (s, 4H), 2.87 (s, 4H), 2.22 (s, 1H), 1.08 (m, 4H). ^{13}C NMR (126 MHz, DMSO-d_6) δ 167.46 (s), 167.30 (s), 162.61 (s), 153.05 (s), 148.80 (s), 133.03 (s), 130.31 (s), 124.18 (s), 123.57 (s), 122.45 (s), 120.98 (s), 117.73 (s), 115.94 (s), 114.71 (s), 50.00 (s), 45.89 (s), 18.55 (s), 10.39 (s). HRMS-EI m/z [M+H] $^{+}$ calcd for $C_{23}H_{25}N_8OS$: 461.1872, found: 461.1861.

4-((2-ethylthieno[2,3-d]pyrimidin-4-yl)amino)-N-(4-(piperazin-1-yl)phenyl)-1H-pyrazole-3-carboxamide (47). Compound **47** was prepared according to general procedure D on 0.5 mmol scale. Purification by column chromatography (5% MeOH/DCM) yield the title compound (63 mg, 0.14 mmol Yield 28%). white solid; m.p 215-216 °C. HPLC analysis: retention time = 3.772 min; peak area, 99.65%. ^{1}H NMR (300 MHz, DMSO-d_6) δ: ^{1}H-NMR (300 MHz, DMSO-d_6) δ 10.11 (d, J = 44.2 Hz, 2H), 8.58 (s, 1H), 7.68 (d, J = 6.4 Hz, 3H), 7.40 (d, J = 5.7 Hz, 1H), 6.92 (d, J = 8.6 Hz, 2H), 3.03 (s, 4H), 2.90 (dd, J = 15.8, 8.1 Hz, 6H), 1.35 (t, J = 7.4 Hz, 3H). ^{13}C-NMR (126 MHz, DMSO-d_6) δ 167.31 (s), 167.23 (s), 162.65 (s), 153.16 (s), 148.87 (s), 133.13 (s), 130.31 (s), 124.26 (s), 124.20 (s), 122.43 (s), 117.73 (s), 115.90 (s), 50.18 (s), 46.03 (s), 32.39 (s), 13.04 (s). HRMS-EI m/z [M+H] $^{+}$ calcd for $C_{22}H_{25}N_8OS$: 449.1872, found: 449.1823.

4-((2-isopropylthieno[2,3-d]pyrimidin-4-yl)amino)-N-(4-(piperazin-1-yl)phenyl)-1H-pyrazole-3-carboxamide (48). Compound **48** was prepared according to general procedure D on 0.5 mmol scale. Purification by column chromatography (5%

MeOH/DCM) yield the title compound (90 mg, 0.20 mmol Yield 39%). white solid; m.p 253-254 °C. HPLC analysis: retention time = 4.252 min; peak area, 98.54%. ^{1}H-NMR (300 MHz, DMSO-d_6) δ 13.56 (s, 1H), 10.27 (s, 1H), 10.03 (s, 1H), 8.58 (s, 1H), 7.73 (dd, *J* = 16.2, 7.0 Hz, 3H), 7.41 (d, *J* = 5.7 Hz, 1H), 7.01 (d, *J* = 8.3 Hz, 2H), 3.19 (dd, *J* = 34.1, 12.7 Hz, 9H), 1.36 (d, *J* = 6.7 Hz, 6H). ^{13}C NMR (126 MHz, DMSO-d_6) δ 170.58 (s), 167.34 (s), 162.76 (s), 158.91 (s), 158.66 (s), 153.25 (s), 147.35 (s), 133.06 (s), 131.39 (s), 124.39 (s), 124.29 (s), 122.45 (s), 117.70 (s), 116.63 (s), 114.87 (s), 47.09 (s), 43.68 (s), 37.43 (s), 22.35 (s). HRMS-EI m/z [M+H] $^{+}$ calcd for $C_{23}H_{27}N_8OS$: 463.2029, found: 163.1983.

4-((2-(tert-butyl)thieno[2,3-d]pyrimidin-4-yl)amino)-N-(4-(piperazin-1-yl)phenyl) -1H-pyrazole-3-carboxamide (49). Compound **49** was prepared according to general procedure D on 0.5 mmol scale. Purification by column chromatography (5% MeOH/DCM) yield the title compound (64 mg, 0.14 mmol Yield 27%). white solid; m.p 229-230 °C. HPLC analysis: retention time =5.131 min; peak area, 98.52%. ^{1}H-NMR (300 MHz, DMSO-d_6) δ13.46 (s, 1H), 10.18 (s, 1H), 10.02 (s, 1H), 8.54 (s, 1H), 7.76 – 7.65 (m, 3H), 7.40 (d, J = 5.9 Hz, 1H), 6.96 (d, J = 8.8 Hz, 2H), 3.16 (s, 4H), 3.03 (s, 4H), 1.44 (s, 9H). ^{13}C-NMR (126 MHz, DMSO-d_6) δ 172.51 (s), 167.29 (s), 162.69 (s), 152.92 (s), 148.03 (s), 132.91 (s), 130.87 (s), 124.53 (s), 124.34 (s), 122.43 (s), 120.93 (s), 117.61 (s), 116.29 (s), 114.56 (s), 48.47 (s), 44.73 (s), 30.26 (s). HRMS-EI m/z [M+H] $^{+}$ calcd for $C_{24}H_{29}N_8OS$: 477.2185, found: 477.2139.

4-((2-methyl-6,7-dihydro-5H-cyclopenta[d]pyrimidin-4-yl)amino)-N-(4-(piperazi n-1-yl)phenyl)-1H-pyrazole-3-carboxamide (50). Compound **50** was prepared

according to general procedure D on 0.5 mmol scale. Purification by column chromatography (5% MeOH/DCM) yield the title compound (67 mg, 0.16 mmol Yield 31%).white solid; m.p 279-280 °C. HPLC analysis: retention time = 3.349 min; peak area, 100.00%. ^{1}H-NMR (600 MHz, DMSO-d_6) δ13.40 (s, 1H), 10.10 (s, 1H), 9.11 (s, 1H), 8.50 (d, J = 14.2 Hz, 1H), 7.67 (d, J = 8.7 Hz, 2H), 6.94 (d, J = 8.5 Hz, 2H), 3.14 (s, 4H), 3.02 (d, J = 2.7 Hz, 4H), 2.78 (dt, J = 13.8, 7.1 Hz, 4H), 2.50 (s, 3H), 2.14 – 2.01 (m, 2H). ^{13}C-NMR (151 MHz, DMSO-d_6) δ 171.88 (s), 165.97 (s), 162.78 (s), 154.97 (s), 148.51 (s), 132.28 (s), 130.55 (s), 125.02 (s), 122.33 (s), 120.28 (s), 116.02 (s), 114.12 (s), 49.62 (s), 45.60 (s), 34.06 (s), 26.32 (s), 26.10 (s), 21.51 (s). HRMS-EI m/z [M+H] $^{+}$ calcd for $C_{22}H_{27}N_8O$: 419.2308, found: 419.2275.

4-((2-methyl-5,6,7,8-tetrahydroquinazolin-4-yl)amino)-N-(4-(piperazin-1-yl)phenyl)-1H-pyrazole-3-carboxamide (51). Compound **51** was prepared according to general procedure D on 0.5 mmol scale. Purification by column chromatography (5% MeOH/DCM) yield the title compound (74 mg, 0.17 mmol Yield 33%). white solid; m.p >290 °C. HPLC analysis: retention time = 3.299 min; peak area, 98.99%. ^{1}H-NMR (600 MHz, DMSO-d_6) δ13.34 (s, 1H), 10.08 (s, 1H), 9.36 (s, 1H), 8.50 (s, 1H), 7.65 (d, J = 9.1 Hz, 2H), 6.93 (d, J = 9.1 Hz, 2H), 3.09 (dd, J = 6.3, 3.4 Hz, 4H), 2.94 (dd, J = 6.2, 3.6 Hz, 4H), 2.61 (t, J = 5.6 Hz, 2H), 2.45 (s, 5H), 1.80 (dd, J = 13.5, 5.8 Hz, 4H). ^{13}C-NMR (151 MHz, DMSO-d_6) δ 163.46 (s), 162.24 (s), 156.78 (s), 147.05 (s), 131.52 (s), 122.39 (s), 116.76 (s), 109.97 (s), 46.42 (s), 43.08 (s), 31.69 (s), 25.92 (s), 22.19 (s), 21.80 (s). HRMS-EI m/z [M+H] $^{+}$ calcd for $C_{23}H_{29}N_8O$: 433.2464, found: 433.2427.

Kinase Inhibition Assay

Activities of kinases were determined using Hot-SpotSM kinase assay which was performed by Reaction Biology Corp. (Malvern PA, USA) as described previously[39].

Cell Growth Inhibition Assay

The human cancer cell lines MV4-11, MOLM-13, MOLT-4, HL-60, K562 and Jurkat were purchased from the American Type Culture Collection (ATCC) (Manassas, VA, USA). The cell lines were maintained in culture media at 37 °C with 5% CO_2. The effects of target compounds on cell proliferation were performed by Nanjin MingJie Biotech Company. Cells were plated in 384-well culture plates (2000-6000/well). Cell proliferation was determined after treatment with compounds for 72 h. Cell viability was measured by Cell Titer-Glo assay (Promega, USA) following manufacturer's instructions, and luminescence was measured in a multilabel reader (Envision2014, PerkinElmer, USA). IC_{50} values were determined by Prism 5.0.

Analysis of P-FLT3, P-STAT5, P-ERK and P-AKT *in Vitro.*

In order to determine levels of P-FLT3, P-STAT5, P-ERK and P-AKT , cells were seeded in a 6-well cell culture plate at a density of 400000 cells per well for MV4-11 in a total volume of 1800 μL, and were incubated overnight in medium containing 10% fetal bovine serum (Life Technologies, Rockville, MD). Then, 200 μL of serially diluted compounds were added to each well. Cell lysates were harvested after 4 h. FLT3/Phospho-FLT3$^{Tyr589/591}$, STAT5/Phospho-STAT5^{Tyr694},

AKT/Phospho-AKT^{Ser473}, ERK/Phosphop44/42MAPK(Erk1/2)$^{Thr202/Tyr204}$ and GAPDH antibody (Cell Signaling Technology) were used for immunoblotting

Apoptosis Assay

The apoptosis of MV4-11 cells was investigated by Annexin V-FITC/PI assay. Cells (2×10^5) were seeded in 6-well plate and were treated with varying concentrations of inhibitor for 24 h. MV4-11 cells were collected and incubated with FITC-conjugated Annexin V. The nuclei were then counterstained with PI. After the dual staining, the cells were screened by a FAC Scan flow cytometer (Millipore Guava EasyCyte 5). Early stage apoptosis cells (Annexin-V-FITC+/PI-, lower right quadrant); latestage apoptosis cells (Annexin-V-FITC+/PI+, upper right quadrant), and necrosis cells (Annexin-V-FITC-/PI+, upper left quadrant).

Metabolic Stability in Liver Microsomes.

The metabolic stability of compound **50** in HLM (human liver microsomes) was tested by Nanjin MingJie Biotech Company. Add 2.5 μL **LT-106-175**, compound **50** or negative control working solution/well to micrisome solution (197.5μL).Then the mixture was incubated at 37°C for 5 min. After addition of NADPH solution (50μL, 5mM), every 30 μL of sample solution was taken out and terminated by a chilled mixture of Tolbutamide and Terfenadine (1:1) at 0, 5, 15, 30 and 60 min, respectively. The mixture was vortexed for 1 min, centrifuged at 4000 rpm for 15 min at 4°C, and the supernatants were analyzed by LC-MS/MS. The data was analyzed by the first order kinetics to calculate $t_{1/2}$ and Cl.

Molecular Modeling

The X-ray crystal structure of CDK2 binding with AT-7519 (PDB code: 2VU3) was retrieved from the Protein Data Bank[40]. The X-ray crystal structure of CDK6 binding with PD-0332991 (PDB code: 2EUF) was retrieved from the Protein Data Bank[41]. The FLT3 DFG-in conformation was obtained from a DFG-peptide modification based on PDB code 1RJB as reported[42].

Compound **LT-106-175** was prepared by using the protein preparation wizard in Maestro with standard settings. Grids of CDK2, CDK6 and FLT3 were generated using Glide, version 10.2, following the standard procedure recommended by Schrodinger. The conformational ensembles were docked flexibly using Glide with standard settings in both standard and extra precision mode. Only poses with low energy conformations and good hydrogen bond geometries were considered.

ASSOCIATED CONTENT

The following files are available free of charge.

^{1}H NMR and ^{13}C NMR spectra for target compounds (.pdf)

Molecular modeling information (.pdb)

AUTHOR INFORMATION

Corresponding Authors

*(Tao Lu) Tel: +86-25-86185180; Fax: +86-25-86185179; E-mail: lut163@163.com

*(Shuai Lu) Tel: +86-25-86185153; Fax: +86-25-86185170; E-mail: lu_shuai@cpu.edu.cn

Author Contributions

The authors declare no competing financial interest. The manuscript was written through contributions of all authors.

ACKNOWLEDGMENT

We are grateful to the National Natural Science Foundation of China (81502925), the Natural Science Foundation of Jiangsu Province (SBK2016020485), the Fundamental Research Funds for the Central Universities (2016ZZD005) and QingLan Project from Jiangsu Province for financial support. Tianren Qin appreciates the College Students Innovation Project for the R&D of Novel Drugs (J1310032) from the National Found for Fostering Talents of Basic Science (NFFTBS). We also express our gratitude to Dr Xiazhong Ren, Dr Huajun Yang, Dr Chunlan Dong (Crown Bioscience Corporation) and Dr Jamie Planck (RBC, Pennsylvania, USA) for their helpful support in biological evaluation. We are grateful to Dr. Hui-fang Li of Chemical Computing Group Inc. and Dr. Feng Zhang of Nanjing University of Chinese Medicine for the critical reading and careful

language modification.

ABBREVIATIONS

CDK, Cyclin-Dependent Kinase; FLT3, Fms-like receptor tyrosine kinase 3; AML, acute myeloid leukemia; GI_{50}, 50% growth inhibition; ara-C ,Cytarabine; RTK, receptor tyrosine kinase; TKI, tyrosine kinase inhibitor; BrdU , 5-bromo-20-deoxyuridine; ITD, internal tandem duplication; Rb, Retinoblastoma; GI, Percentage of tumor growth inhibition; PTR, Percent tumor regression.

Reference

[1] P.J. Fialkow, J.W. Singer, W.H. Raskind, J.W. Adamson, R.J. Jacobson, I.D. Bernstein, L.W. Dow, V. Najfeld, R. Veith, Clonal development, stem-cell differentiation, and clinical remissions in acute nonlymphocytic leukemia, New England Journal of Medicine, 317 (1987) 468-473.

[2] J. Meyers, Y. Yu, J.A. Kaye, K.L. Davis, Medicare fee-for-service enrollees with primary acute myeloid leukemia: an analysis of treatment patterns, survival, and healthcare resource utilization and costs, Applied Health Economics & Health Policy, 11 (2013) 275-286.

[3] D.L. Stirewalt, J.P. Radich, The role of FLT3 in haematopoietic malignancies, Nature Reviews Cancer, 3 (2003) 650.

[4] F. Birg, M. Courcoul, O. Rosnet, F. Bardin, M.J. Pébusque, S. Marchetto, A. Tabilio, P. Mannoni, D. Birnbaum, Expression of the FMS/KIT-like gene FLT3 in human acute leukemias of the myeloid and lymphoid lineages, Blood, 80 (1992) 2584-2593.

[5] F. Birg, N. Carbuccia, O. Rosnet, D. Birnbaumt, The Expression of FMS, KIT and FLT3 in Hematopoietic Malignancies, Leukemia & Lymphoma, 13 (1994) 223.

[6] C.E. Carow, M. Levenstein, S.H. Kaufmann, J. Chen, S. Amin, P. Rockwell, L. Witte, M.J. Borowitz, C.I. Civin, D. Small, Expression of the hematopoietic growth factor receptor FLT3 (STK-1/Flk2) in human leukemias, Blood, 87 (1996) 1089.

[7] D.G. Gilliland, J.D. Griffin, The roles of FLT3 in hematopoiesis and leukemia, Blood, 100 (2002) 1532-1542.

[8] Y. Yamamoto, H. Kiyoi, Y. Nakano, R. Suzuki, Y. Kodera, S. Miyawaki, N. Asou, K. Kuriyama, F. Yagasaki, C. Shimazaki, Activating mutation of D835 within the activation loop of FLT3 in human hematologic malignancies, Blood, 97 (2001) 2434-2439.

[9] F.M. Abuduhier, A.C. Goodeve, G.A. Wilson, R.S. Care, I.R. Peake, J.T. Reilly, Identification of novel FLT-3 Asp835 mutations in adult acute myeloid leukaemia, British Journal of Haematology, 113 (2001) 983.

[10] S. Fröhling, R.F. Schlenk, J. Breitruck, A. Benner, S. Kreitmeier, K. Tobis, H. Döhner, K. Döhner, Prognostic significance of activating FLT3 mutations in younger adults (16 to 60 years) with acute myeloid leukemia and normal cytogenetics: a study of the AML Study Group Ulm, 100 (2002) 4372-4380.

[11] U. Bacher, C. Haferlach, W. Kern, T. Haferlach, S. Schnittger, Prognostic relevance of FLT3-TKD mutations in AML: the combination matters--an analysis of 3082 patients, Blood, 111 (2008) 2527.

[12] S.P. Whitman, A.S. Ruppert, M.D. Radmacher, K. Mrózek, P. Paschka, C. Langer, C.D. Baldus, J. Wen, F. Racke, B.L. Powell, FLT3 D835/I836 mutations are associated with poor disease-free survival and a distinct gene-expression signature among younger adults with de novo cytogenetically normal acute myeloid leukemia lacking FLT3 internal tandem duplications, Blood, 111 (2008) 1552.

[13] Kiyoi H; Naoe T; Nakano Y; Yokota S; Minami S; Miyawaki S; Asou N; Kuriyama K; Jinnai I; Shimazaki C; Akiyama H; Saito K; Oh H; Motoji T; Omoto E; Saito H; Ohno R; Ueda R. Prognostic implication of FLT3 and N-RAS gene mutations in acute myeloid leukemia.[J]. Blood, 1999, 93(9):3074-3080, Prognostic implication of FLT3 and N-RAS gene mutations in acute myeloid leukemia, Blood, 93 (1999) 3074-3080.

[14] P.D. Kottaridis, R.E. Gale, M.E. Frew, G. Harrison, S.E. Langabeer, A.A. Belton, H. Walker, K. Wheatley, D.T. Bowen, A.K. Burnett, The presence of a FLT3 internal tandem duplication in patients with acute myeloid leukemia (AML) adds important prognostic information to cytogenetic risk group

and response to the first cycle of chemotherapy: analysis of 854 patients from the United Kingd, Blood, 98 (2001) 1752.

[15] Q. Lan, Y. Zhi, H. Heng, X. Guo, H. Liu, Y. Chen, T. Lu, S. Lu, Chemical Space of FLT3 Inhibitors as the Potential Anti-AML Drugs, Recent patents on anti-cancer drug discovery, 12 (2017).

[16] W. Fiedler, S. Kayser, M. Kebenko, M. Janning, J. Krauter, M. Schittenhelm, K. Götze, D. Weber, G. Göhring, V. Teleanu, A phase I/II study of sunitinib and intensive chemotherapy in patients over 60 years of age with acute myeloid leukaemia and activating FLT3 mutations, Br J Haematol, 169 (2015) 694-700.

[17] M. Levis, F. Ravandi, E.S. Wang, M.R. Baer, A. Perl, S. Coutre, H. Erba, R.K. Stuart, M. Baccarani, L.D. Cripe, Results from a randomized trial of salvage chemotherapy followed by lestaurtinib for patients with FLT3 mutant AML in first relapse, Blood, 117 (2011) 3294-3301.

[18] D.J. Deangelo, R.M. Stone, M.L. Heaney, S.D. Nimer, R.L. Paquette, R.B. Klisovic, M.A. Caligiuri, M.R. Cooper, J.M. Lecerf, M.D. Karol, Phase 1 clinical results with tandutinib (MLN518), a novel FLT3 antagonist, in patients with acute myelogenous leukemia or high-risk myelodysplastic syndrome: safety, pharmacokinetics, and pharmacodynamics, Blood, 108 (2006) 3674.

[19] S. Knapper, The clinical development of FLT3 inhibitors in acute myeloid leukemia, Expert Opinion on Investigational Drugs, 20 (2011) 1377-1395.

[20] M. Larrosa-Garcia, M.R. Baer, FLT3 Inhibitors in Acute Myeloid Leukemia: Current Status and Future Directions, Molecular Cancer Therapeutics, 16 (2017) 991-1001.

[21] E.S. Kim, Midostaurin: First Global Approval, Drugs, 77 (2017) 1-9.

[22] P.P. Zarrinkar, M.D. Gunawardane RNCramer, AC220 is a uniquely potent and selective inhibitor of FLT3 for the treatment of acute myeloid leukemia (AML), Blood, 114 (2009) 2984.

[23] A. Galanis, M. Levis, Inhibition of c-Kit by tyrosine kinase inhibitors, Haematologica, 100 (2015) 77-79.

[24] C.C. Smith, Q. Wang, C.S. Chin, S. Salerno, L.E. Damon, M.J. Levis, A.E. Perl, K.J. Travers, S. Wang, J.P. Hunt, Validation of ITD mutations in FLT3 as a therapeutic target in human acute myeloid leukaemia, Nature, 485 (2012) 260-263.

[25] P.G. Wyatt, A.J. Woodhead, V. Berdini, J.A. Boulstridge, M.G. Carr, D.M. Cross, D.J. Davis, L.A. Devine, T.R. Early, R.E. Feltell, E.J. Lewis, R.L. McMenamin, E.F. Navarro, M.A. O'Brien, M. O'Reilly, M. Reule, G. Saxty, L.C. Seavers, D.M. Smith, M.S. Squires, G. Trewartha, M.T. Walker, A.J. Woolford, Identification of N-(4-piperidinyl)-4-(2,6-dichlorobenzoylamino)-1H-pyrazole-3-carboxamide (AT7519), a novel cyclin dependent kinase inhibitor using fragment-based X-ray crystallography and structure based drug design, J Med Chem, 51 (2008) 4986-4999.

[26] Y. Lu, T. Ran, G. Lin, Q. Jin, J. Jin, H. Li, H. Guo, T. Lu, Y. Wang, Novel 1H-pyrazole-3-carboxamide derivatives: synthesis, anticancer evaluation and identification of their DNA-binding interaction, Chemical & Pharmaceutical Bulletin, 62 (2014) 238-246.

[27] H. Lu, U. Schulze-Gahmen, Toward understanding the structural basis of cyclin-dependent kinase 6 specific inhibition, Journal of Medicinal Chemistry, 49 (2006) 3826.

[28] T. Shimamura, J. Shibata, H. Kurihara, T. Mita, S. Otsuki, T. Sagara, H. Hirai, Y. Iwasawa, Identification of Potent 5‐Pyrimidinyl‐2‐aminothiazole CDK4, 6 Inhibitors with Significant Selectivity over CDK1, 2, 5, 7, and 9, Bioorganic & Medicinal Chemistry Letters, 16 (2006) 3751-3754.

[29] S.R. Whittaker, A. Mallinger, P. Workman, P.A. Clarke, Inhibitors of cyclin-dependent kinases as cancer therapeutics, Pharmacology & Therapeutics, 173 (2017).

[30] L. Z, W. X, J. Eksterowicz, G.M. Jr, A. GQ, A. M, C. TJ, C. A, C. X, C. R, Discovery of AMG 925, a FLT3

and CDK4 Dual Kinase Inhibitor with Preferential Affinity for the Activated State of FLT3, 57 (2014) 3430-3449.

[31] M.R. Wood, M.J. Noetzel, J.L. Engers, K.A. Bollinger, B.J. Melancon, J.C. Tarr, C. Han, M. West, A.R. Gregro, A. Lamsal, Discovery and optimization of a novel series of highly CNS penetrant M4 PAMs based on a 5,6-dimethyl-4-(piperidin-1-yl)thieno[2,3-d] pyrimidine core, Bioorganic & Medicinal Chemistry Letters, 26 (2016) 3029-3033.

[32] B.C. Shook, D. Chakravarty, J.K. Barbay, A. Wang, K. Leonard, V. Alford, M.T. Powell, S. Rassnick, R.H. Scannevin, K. Carroll, Substituted thieno[2,3-d]pyrimidines as adenosine A2A receptor antagonists, Bioorganic & Medicinal Chemistry Letters, 23 (2013) 2688-2691.

[33] P.P. Zarrinkar, R.N. Gunawardane, M.D. Cramer, M.F. Gardner, D. Brigham, B. Belli, M.W. Karaman, K.W. Pratz, G. Pallares, Q. Chao, AC220 is a uniquely potent and selective inhibitor of FLT3 for the treatment of acute myeloid leukemia (AML), Blood, 114 (2009) 2984.

[34] Smith CC, Zhang C, Lin KC, Lasater EA, Zhang Y, Massi E, Damon LE, Pendleton M, Bashir A, Sebra R, Perl A, Kasarskis A, Shellooe R, Tsang G, Carias H, Powell B, Burton EA, Matusow B, Zhang J, Spevak W, Ibrahim PN, Le MH, Hsu HH, Habets G, West BL, Bollag G, Shah NP. Characterizing and Overriding the Structural Mechanism of the Quizartinib-Resistant FLT3 "Gatekeeper" F691L Mutation with PLX3397, Cancer Discovery, 5 (2015) 668.

[35] A.A. Warkentin, M.S. Lopez, E.A. Lasater, K. Lin, B.L. He, A.Y. Leung, C.C. Smith, N.P. Shah, K.M. Shokat, Overcoming myelosuppression due to synthetic lethal toxicity for FLT3-targeted acute myeloid leukemia therapy, 3 (2014).

[36] J.M. Hatcher, E. Weisberg, T. Sim, R.M. Stone, S. Liu, J.D. Griffin, N.S. Gray, Discovery of a Highly Potent and Selective Indenoindolone Type 1 Pan-FLT3 Inhibitor, Acs Medicinal Chemistry Letters, 7 (2016) 476.

[37] H. Kiyoi, FLT3 INHIBITORS: RECENT ADVANCES AND PROBLEMS FOR CLINICAL APPLICATION, Nagoya Journal of Medical Science, 77 (2015) 7-17.

[38] K.M. Kampaschittenhelm, M.C. Heinrich, F. Akmut, H. Döhner, K. Döhner, M.M. Schittenhelm, Quizartinib (AC220) is a potent second generation class III tyrosine kinase inhibitor that displays a distinct inhibition profile against mutant- FLT3, -PDGFRA and - KIT isoforms, Molecular Cancer, 12 (2013) 19.

[39] W. Yang, Y. Chen, X. Zhou, Y. Gu, W. Qian, F. Zhang, W. Han, T. Lu, W. Tang, Design, synthesis and biological evaluation of bis-aryl ureas and amides based on 2-amino-3-purinylpyridine scaffold as DFG-out B-Raf kinase inhibitors, European journal of medicinal chemistry, 89 (2015) 581-596.

[40] P.G. Wyatt, A.J. Woodhead, V. Berdini, J.A. Boulstridge, M.G. Carr, D.M. Cross, D.J. Davis, L.A. Devine, T.R. Early, R.E. Feltell, Identification of N-(4-piperidinyl)-4-(2,6-dichlorobenzoylamino)-1H-pyrazole-3-carboxamide (AT7519), a novel cyclin dependent kinase inhibitor using fragment-based X-ray crystallography and structure based drug design, Journal of Medicinal Chemistry, 51 (2008) 4986-4999.

[41] H.L. And, Ursula Schulzegahmen, Toward Understanding the Structural Basis of Cyclin-Dependent Kinase 6 Specific Inhibition, Journal of Medicinal Chemistry, 49 (2006) 3826.

[42] V. Hornak, R.A. Abel, B. Strockbine, A. Roitberg, C. Simmerling, Comparison of multiple Amber force fields and development of improved protein backbone parameters, Proteins Structure Function & Bioinformatics, 65 (2006) 712-725.

Highlights:

- A selective FLT3 inhibitor was discovered through structure-based molecular design to reduce the CDK inhibitory potency of lead compound.
- Compound **50** was highly potent aganist FLT3 as well as a variety of FLT3 mutants including the potential drug-resistance forms, FLT3 (ITD)-D835V and FLT3 (ITD)-F691L.
- Compound **50** showed subnanomolar cell growth inhibitory activity in MV4-11 cell line.